European Review for Medical and Pharmacological Sciences 2015; 19: 1013-1021

Decreased CUL4B expression inhibits malignant proliferation of glioma *in vitro* and *in vivo*

J. DONG[1,3], X.-Q. WANG[1,3], J.-J. YAO[2], G. LI[1], X.-G. LI[1]

[1]Department of Neurosurgery, Qilu Hospital of Shandong University and Brain Science Research Institute, Shandong University, Jinan, China
[2]Department of Gastroenterology, People Hospital of Rizhao City, Rizhao, China
[3]Department of Neurosurgery, People Hospital of Rizhao City, Rizhao, China

Jun Dong and *Xing-Qiang Wang* contributed equally to this work

Abstract. – OBJECTIVE: Cullin 4B (CUL4B) is a component of the Cullin 4B-Ring E3 ligase complex (CRL4B) that plays a role in proteolysis and is implicated in tumorigenesis. However, little is known about CUL4B function in human brain tumors, including glioma.

MATERIALS AND METHODS: Here, to investigate the involvement of CUL4B in glioma tumorigenesis, endogenous CUL4B expression was depleted in glioblastoma cell lines U87 and U251 by RNA interference (RNAi).

RESULTS: Knockdown of CUL4B via shRNA-delivering lentiviruses significantly decreased cell proliferation and colony formation, causing G1 phase cell cycle arrest in both cell lines via down-regulation of cyclin D1 and up-regulation of p16. While increasing the expression of the tumor suppressor PTEN, CUL4B knockdown alleviated *in vivo* tumorigenesis in glioma xenograft nude mice and impeded cell migration via suppression of MMP-9.

CONCLUSIONS: Therefore, knockdown of CUL4B is likely to provide a novel alternative for targeted therapy of glioma deserving further investigation.

Key Words:
Cullin 4B, Glioma, shRNA, Proliferation, Cell cycle, Tumorigenesis.

Introduction

Gliomas are the most common primary tumors of the adult central nervous system (CNS), characterized by high morbidity and mortality as well as a high recurrence rate[1]. Presumably, gliomas arise from mature glia or neural stem cells and diffusely infiltrate surrounding tissues[2], complicating surgical resection. Survival from gliomas depends on tumor type and grade of malignancy[3]. According to World Health Organization (WHO) standards, gliomas are classified into four malignant grades (I, II, III, IV). The most lethal is grade IV glioblastoma (GBM), with a five-year survival rate of less than 10% due to difficulties in complete resection and low sensitivity to radio- and chemotherapy[4-6]. Thus, treatment of gliomas remains one of the most disappointing challenges in modern oncology.

Cullin 4B (CUL4B), a scaffold protein that assembles the CRL4B ubiquitin ligase complex, participates in the regulation of a broad spectrum of biological processes. CUL4B binds to UV-damaged chromatin via DDB2, it may be important for DNA repair and replication[7,8], and it regulates the mTOR pathway involved in control of cell growth, size, and metabolism[9]. Previous studies[10] demonstrated that CUL4B expression is markedly upregulated in various human cancers, promoting cell proliferation, invasion, and tumorigenesis. While Jiang et al[11] demonstrated that CUL4B is a novel prognostic marker correlating with colon cancer pathogenesis and progression, CUL4B was also reported to promote proliferation and inhibit apoptosis of osteosarcoma cells[12].

CUL4B mutations were found to cause human X-linked mental retardation (XLMR) syndrome, associated with aggressive outbursts, seizures, relative macrocephaly, central obesity, hypogonadism, pes cavus, and tremor[13-16]. The unique CUL4B N-terminus may mediate the recruitment of distinct substrates for degradation, and their accumulation may contribute to the CUL4B phenotype. XLMR-linked CUL4B mutations resulted in the accumulation of WDR5, a subunit of the H3K4 methyltransferase complex, and subsequent activation of neuronal genes promoting

Corresponding Author: Xin-Gang Li, MD; e-mail: lxgang_lxg@163.com; Gang Li, MD; e-mail: lixg@sdu.edu.cn

neurite extension[17]. Peroxiredoxin III is another unique CUL4B substrate that may affect neural development through the regulation of reactive oxygen species (ROS) levels[18]. A recent report showed that the phenotypic heterogeneity of cerebral malformations might result from the involvement of CUL4B in various cellular pathways essential for normal brain development[19].

Whereas CUL4B is involved in the pathogenesis of human malignancy and neuronal disease, its exact role in primary brain tumors such as gliomas has not yet been determined. Here, we assessed expression levels of CUL4B in human glioma samples and used specific small interfering RNA (siRNA) to downregulate CUL4B expression and investigate its impact on growth in U87 and U251 glioblastoma cells *in vitro* and *in vivo*.

Materials and Methods

Cell Culture

Human glioblastoma cell lines U87 and U251 and the human embryonic kidney cell line 293T were obtained from the Cell Bank of the Chinese Academy of Sciences (Shanghai, China). All cell lines were maintained in Dulbecco's modified Eagle's medium (DMEM; Logan, UT, USA) supplemented with 10% fetal bovine serum (FBS; Loire Valley, France) at 37°C in a 5% CO_2 humidified incubator.

Real-time Quantitative PCR

Total RNA was extracted from glioma tissues and cultured cell lines using TRIzol® reagent (Invitrogen, Carlsbad, CA, USA), and cDNA was synthesized using M-MLV reverse transcriptase (Promega, Madison, WI, USA). Real-time quantitative PCR (qPCR) was carried out on an ABI PRISM 7000 Sequence Detection System (Applied Biosystems, Foster City, CA, USA) according to the manufacturer's protocol, briefly, denaturation at 95°C for 1 min, 40 cycles of denaturation at 95°C for 5 s and extension at 60°C for 20 s. The β-actin gene was amplified as an internal control. The following primers were used: CUL4B, 5'-TGGAAGTTCATTTACCACCAGAGATG-3' (forward) and 5'-TTCTGCTTTTAACACACAGTGTCCTA-3' (reverse); β-actin, 5′-GTGGACATCCGCAAAGAC-3′ (forward) and 5′-AAAGGGTGTAACGCAACTA-3′ (reverse). For relative quantification of gene expression, the $2^{-\Delta\Delta CT}$ method was used.

Construction of CUL4B siRNA-Containing Lentiviruses and Transduction Into Glioma Cells

The siRNA sequence 5'-AGCAGTGGAAGCTATTCAGAA-3' was designed to knock down the expression of the human CUL4B gene, and the siRNA sequence 5'-TTCTCCGAACGTGTCACGT-3' was used as a control. A stem-loop-stem oligonucleotide (short hairpin RNA, shRNA) corresponding to each siRNA was inserted into the pGCSIL-GFP vector (Genechem, Shanghai, China). Recombinant lentiviruses were produced by co-transfecting 293T cells with the lentivirus expression vector and packaging plasmids pHelper 1.0 and pHelper 2.0 (Genechem) using Lipofectamine 2000 (Invitrogen). Supernatants were collected 48 h after transfection, and lentiviral particles were purified by ultracentrifugation (4,000 × *g*) at 4°C for 10 min.

For infection, U87 and U251 cells (50,000 cells/well) were seeded in 6-well plates and transduced with the constructed lentiviruses containing CUL4B shRNA (Lv-shCUL4B) or non-silencing shRNA(Lv-shCon) at a multiplicity of infection (MOI) of 20. Green fluorescent protein (GFP) encoded by the lentiviral vectors was used to assess infection efficiency in transduced cells.

Western Blot

Five days after lentivirus infection, U87 and U251 cells, respectively, were washed twice with PBS and suspended in lysis buffer (2% mercaptoethanol, 20% glycerol, 4% SDS in 100 mM Tris-HCl, pH 6.8). Protein concentrations were determined using a BCA Protein Assay Kit (Beyotime, Shanghai, China). β-actin protein served as a loading control. Equal amounts (30 μg) of protein samples were separated by SDS-PAGE and transferred to polyvinylidene difluoride (PVDF) membranes (Millipore, Bedford, MA, USA). Nonspecific binding was blocked by incubation in TBST (25 mM Tris, pH 7.4, 150 mM NaCl, 0.1% Tween-20) containing 5% skimmed milk at room temperature for 1 h. Membranes were incubated with primary antibodies at 4°C overnight, followed by horseradish peroxidase (HRP)-conjugated secondary antibodies at room temperature for 1 h. Bands were visualized after incubation with chemiluminescence detection reagent (Pierce, Rockford, IL, USA).

Rabbit anti-CUL4B (#10-P1233) antibody was obtained from American Research Products (Waltham, MA, USA); mouse anti-cyclin D1 (#MD-17-3) antibody was from Medical & Bio-

logical Laboratories (Aichi, Japan); rabbit anti-p16INK4a (#4824), rabbit anti-MMP-9 (#2270), rabbit anti-PTEN (#7960), and rabbit anti-β-actin (#4967) antibodies were from Cell Signaling Technology (Danvers, MA, USA); HRP-conjugated goat anti-rabbit (#SC-2054) and goat anti-mouse (#SC-2005) secondary antibodies were from Santa Cruz Biotechnology (Dallas, TX, USA).

Cell Proliferation Assay

After lentivirus infection, U87 and U251 cells (2,000 cells/well), respectively, were reseeded in 96-well plates and incubated at 37°C for 1, 2, 3, 4, and 5 days, respectively. At termination of culture, cell proliferation was analyzed using the Cell Counting Kit-8 (CCK-8; Dojindo Laboratories, Japan) according to the manufacturer's instructions. After incubation at 37°C for 2 h, absorbance was measured at 450 nm using an iMark microplate reader (Bio-Rad, Hercules, CA, USA).

Colony Formation Assay

After lentivirus infection, U87 and U251 cells (500 cells/well), respectively, were reseeded in 6-well plates and incubated for 8 days to form normal colonies. The medium was replaced every 3 days, cells were washed with PBS and fixed with 4% paraformaldehyde for 30 min. Fixed cells were stained with freshly prepared crystal violet (Beyotime) for 20 min, and colonies were counted under a microscope.

Cell Cycle Analysis

Cell cycle distribution was analyzed by flow cytometry using propidium iodide (PI) staining. Four days after lentivirus infection, U87 and U251 cells, respectively, were reseeded in 6-cm dishes at a density of 200,000 cells/dish. After culture at 37°C for 40 h, cells were harvested, fixed in 70% ethanol, stored at 4°C overnight, stained with NaCl/PI solution containing 50 μg/mL PI and 100 μg/mL RNase A in the dark at room temperature for 1 h, and analyzed by flow cytometry (FACSCalibur; Becton Dickinson, San Jose, CA, USA). Fractions of cells in G0/G1, S, and G2/M phases were analyzed using dedicated software (Becton Dickinson).

Transwell Assay

Cell migration was examined using Transwell chambers (8.0-μm pores, 24 wells; Corning Costar, Corning, NY, USA). Four days after lentivirus infection, U87 and U251 cells were reseeded in upper chambers at a concentration of 50,000 and 30,000 cells/well, respectively, in 200 μL serum-free DMEM, and upper chambers were filled with DMEM containing 10% FBS. After incubation at 37°C for 24 h, non-migrated cells on the upper surface of the filter were gently removed using cotton swabs, while migrated cells on the lower surface were fixed with 4% paraformaldehyde, stained with crystal violet, and counted (five random fields per well) under a microscope.

In vivo Tumorigenesis

Sixteen 6-week old female BALB/c nude mice (body weight 20.0 ± 2.5 g) were obtained from Beijing HFK Bioscience Co., Ltd. (Beijing, China) and kept under specific pathogen-free (SPF) conditions. All animal experiments were evaluated and approved by the Ethics Committee of Qilu Hospital and the Brain Science Research Institute of Shandong University.

After lentivirus infection, U87 and U251 cells were collected and washed with serum-free DMEM. Sixteen nude mice were randomly assigned to four groups of four and injected with treated U87 or U251 cells (5×10^5 cells/site) into the back of the neck. Diameters of tumors in the greatest axis (a) and shortest axis (b) were measured using a vernier caliper every 3-4 days, and tumor volumes were calculated using the following formula: tumor volume (mm^3) = $1/2\ (a \times b^2)$. Tumor growth was followed for 3 weeks after the first injection, mice were sacrificed by cervical dislocation, and tumors were excised for weighing.

Statistical Analysis

For statistical analysis, the SPSS 16.0 software package (SPSS Inc., Chicago, IL, USA) was used. All data were expressed as mean ± standard deviation (SD). Differences between two groups were analyzed by Student's *t*-test, and a *p*-value of < 0.05 was considered statistically significant.

Results

Expression of CUL4B in Glioma and Adjacent Brain Tissues

To explore the role of CUL4B in human glioma, we evaluated its expression in 15 paired glioma and adjacent brain tissues by qPCR. Figure 1 shows that in two thirds of glioma tissues

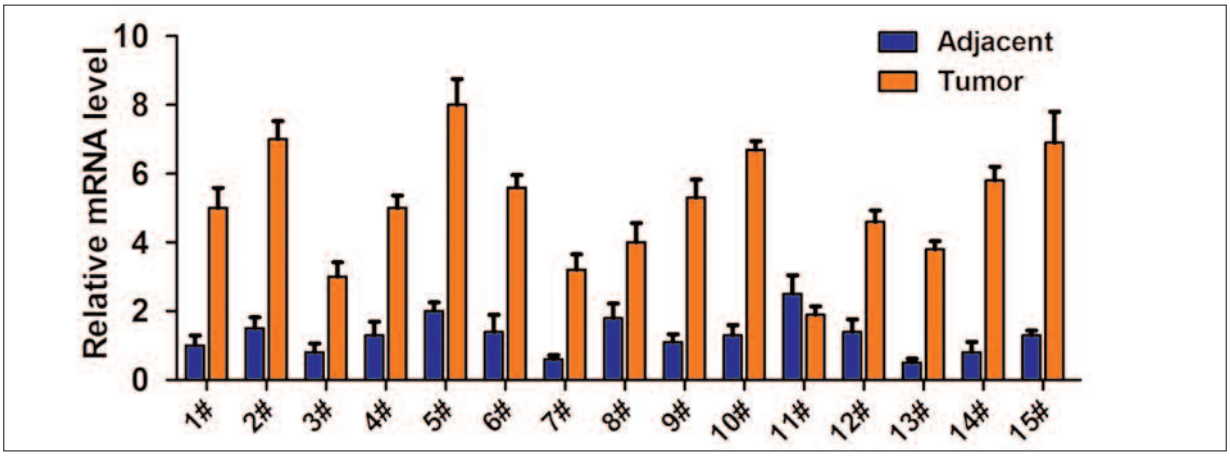

Figure 1. Expression patterns of CUL4B in glioma and adjacent brain tissues. qPCR analysis of CUL4B expression in 15 paired glioma and adjacent brain tissue samples.

CUL4B mRNA levels were increased more than three-fold compared to matched normal tissues. These results indicate that CUL4B is highly expressed in glioma tissues and might be associated with glioma development.

Knockdown of CUL4B in Glioblastoma Cells by Lentivirus-Mediated shRNA

U87 and U251 cells were transduced with shRNA-delivering lentiviruses (Lv-shCon or Lv-shCUL4B). GFP expression was detected by fluorescent microscopy four days post-infection. As shown in Figure 2A, over 80% of cells in both the Lv-shCon and Lv-shCUL4B groups expressed GFP, indicating a high infection rate of the cell lines. Inhibitory effects of Lv-shCUL4B on endogenous CUL4B expression were examined by qPCR and western blot. As shown in Figure 2B and D, CUL4B mRNA levels were reduced by 77.4% and 77.8% in Lv-shCUL4B-

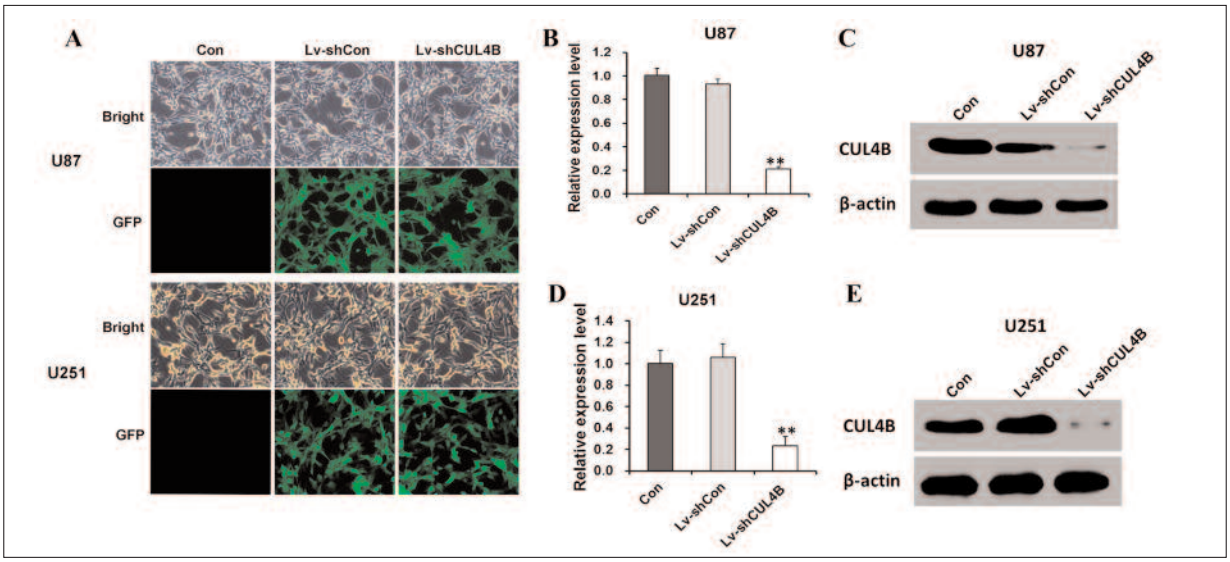

Figure 2. CUL4B expression depleted by lentivirus-delivered shRNA. ***A,*** GFP expression in lentivirus-infected U87 and U251 cells (compared to uninfected controls) detected by fluorescence microscopy. ***B,*** and ***D,*** qPCR analysis of CUL4B knockdown efficiency comparing uninfected and lentivirus-infected U87 and U251 cells. The β-actin gene was used as internal control. ***C,*** and ***E,*** Representative western blot demonstrating CUL4B knockdown efficiency by comparing uninfected and lentivirus-infected U87 and U251 cells. GAPDH protein was used as internal control. Data are mean ± SD. (n = 3; *t*-test). $^{**}p < 0.01$.

transduced U87 and U251 cells, respectively, compared to Lv-shCon and Con (uninfected) controls, which were not significantly different from each other. Western blot data verified the down-regulation of CUL4B expression in both cell lines (Figure 2C and E). Therefore, lentivirus-delivered shRNA could specifically deplete endogenous CUL4B expression in glioblastoma cells.

Effects of CUL4B Knockdown on Cell Proliferation and Colony Formation

To evaluate the effects of CUL4B on glioma cell proliferation, CCK-8 assays were performed with U87 and U251 cells after lentivirus infection. As shown in Figure 3A and 3B, proliferation rates were reduced by 63.7% in U87 cells and 45.5% in U251 cells on day 5 after transduction with Lv-shCUL4B, compared to controls. These results indicate that knockdown of CUL4B can strongly reduce the proliferation of glioblastoma cells.

Moreover, colony formation assays were performed with U87 and U251 cells after lentivirus infection, and representative photographs of crystal violet-stained colonies per well were taken (Figure 3C). While the average numbers of total colonies were nearly 150 or 200 in controls (Con and Lv-shCon), there were less than 30 or 40 colonies of Lv-shCUL4B-transduced U87 or U251 cells, respectively (Figure 3D and E). These results indicate that knockdown of CUL4B can strongly disrupt colony formation of glioblastoma cells.

Effects of CUL4B Knockdown on Cell Cycle Control

To assess the mechanism by which CUL4B modulates cell proliferation, flow cytometry assays were used to determine cell cycle distribu-

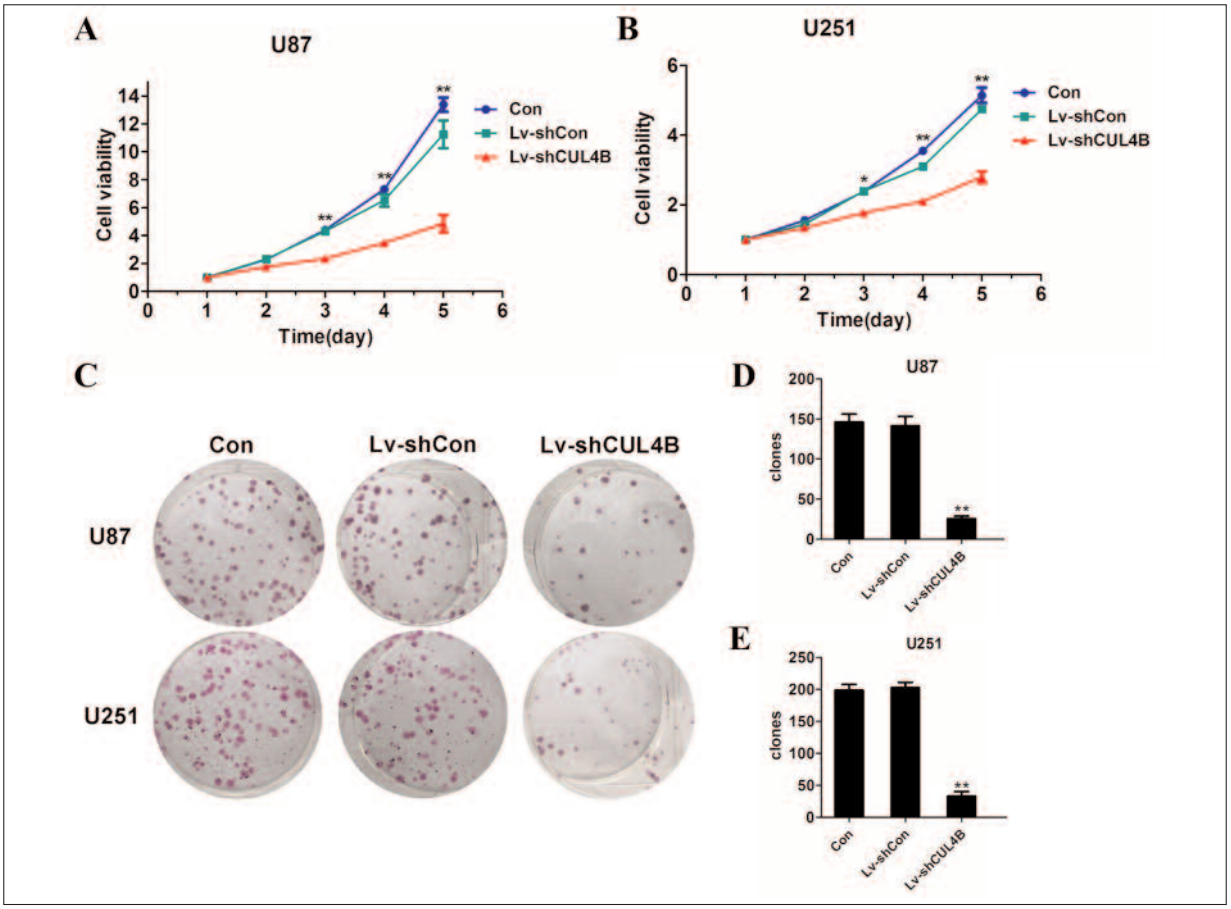

Figure 3. Depletion of CUL4B decreased cell proliferation and colony formation. ***A,*** and ***B,*** Growth curves of uninfected and lentivirus-infected U87 and U251 cell lines determined by cell proliferation assays. ***C,*** Representative colony formation showing clonogenic survival of uninfected and lentivirus-infected U87 and U251 cell lines. ***D,*** and ***E,*** Statistical analysis of colony numbers of uninfected and lentivirus-infected U87 and U251 cell lines. Data are mean ± SD. (n = 3; *t*-test). *$p < 0.05$, ** $p < 0.01$.

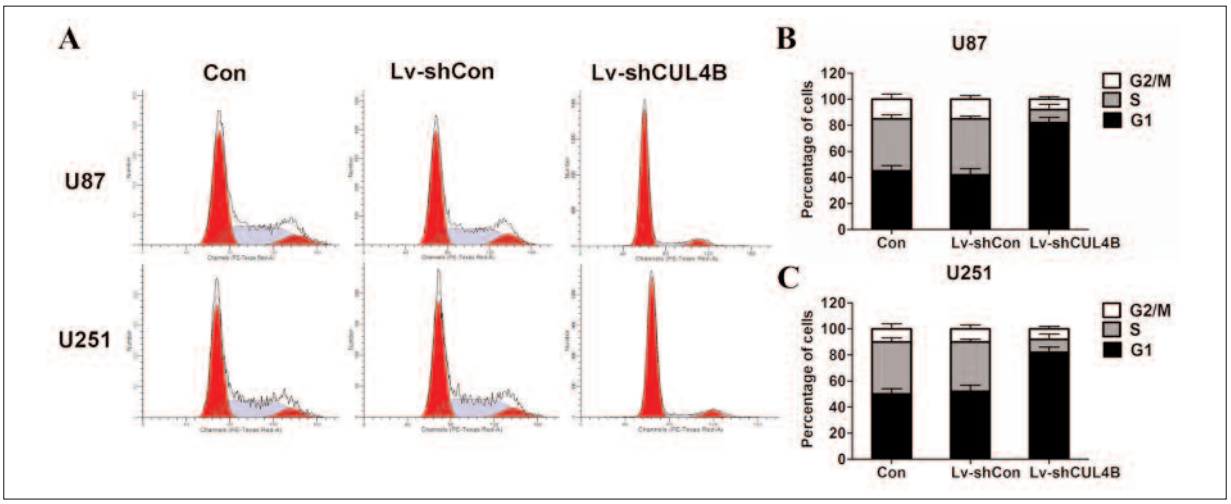

Figure 4. G1 phase cell cycle arrest induced by depletion of CUL4B. ***A,*** Flow cytometry analysis of cell cycle distributions in uninfected and lentivirus-infected U87 and U251 cell lines. ***B,*** and ***C,*** Statistical analysis of G1, S, and G2/M phase populations in uninfected and lentivirus-infected U87 and U251 cell lines. Data are mean ± SD. (n = 3; *t*-test).

tions in U87 and U251 cells (Figure 4A). As shown in Figure 4B, the percentage of cells in G1 phase was increased from approximately 50.0% or 52.0% in controls (Con or Lv-shCon, respectively) to 82.0% in Lv-shCUL4B-transduced U87 cells. In contrast, the percentage of cells in S phase was decreased from about 40.0% or 38.0% in controls (Con or Lv-shCon, respectively) to 10.0% in Lv-shCUL4B-transduced U87 cells. Similarly, percentages of U251 cells in G1 phase were increased and percentages in S phase were decreased in response to CUL4B knockdown (Figure 4C). These results indicate that knockdown of CUL4B can inhibit glioblastoma cell proliferation by inducing G1 phase cell cycle arrest.

Effects of CUL4B Knockdown on Cell Migration

Furthermore, we examined the effects of CUL4B on glioblastoma cell migration using Transwell chambers. Representative images of U87 and U251 cells that migrated to the lower surface are presented in Figure 5A. The average number of migrated Lv-shCUL4B-transduced U87 cells was 65, representing a significant reduction from 224 and 210 in controls (Con and Lv-shCon, respectively; $p < 0.01$, Figure 5B). Similarly, numbers of migrated U251 cells were significantly reduced by CUL4B knockdown ($p < 0.01$, Figure 5C). These results indicate that knockdown of CUL4B can alleviate migration of glioblastoma cells.

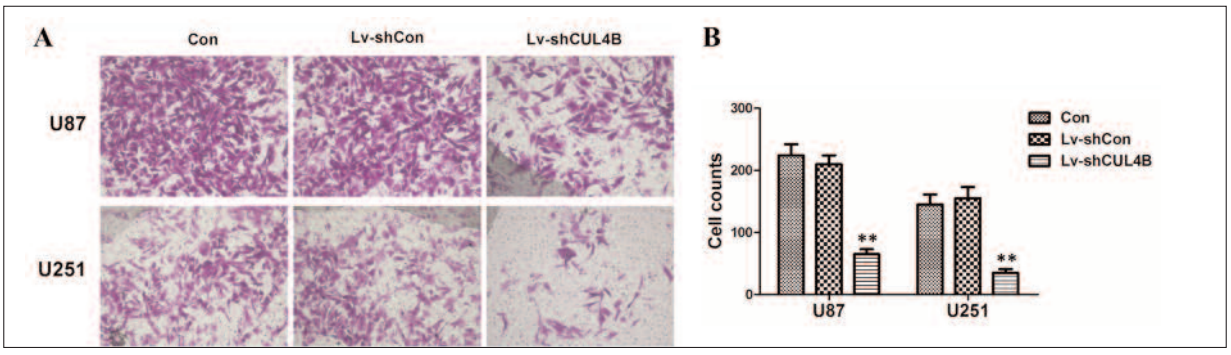

Figure 5. Cell migration impeded by depletion of CUL4B. ***A,*** Representative crystal violet staining showing cell migration in uninfected and lentivirus-infected U87 and U251 cell lines. ***B,*** and ***C,*** Statistical analysis of migrated cells in uninfected and lentivirus-infected U87 and U251 cell lines. Data are mean ± SD (n = 3; t-test). ** $p < 0.01$.

Effects of CUL4B Knockdown on Regulators of Cell Cycle and Migration

To survey the molecular mechanisms underlying CUL4B-mediated cell growth and migration, alterations in the expression of some regulators associated with cell cycle and motility were analyzed in U87 and U251 cells using western blot. As shown in Figure 6, the expression levels of cyclin D1 and MMP-9 were obviously down-regulated, while p16INK4a and PTEN were up-regulated in Lv-shCUL4B-transduced cells compared with controls (Con and Lv-shCon). These results indicate that CUL4B might play an essential role in glioma growth and metastasis by modifying the expression patterns of regulatory proteins.

Effects of CUL4B Knockdown on Yumor Growth in vivo

A human xenograft nude mouse model of glioma was used with lentivirus-infected U87 or U251 cells. With increasing time after implantation, tumor volumes in all groups would progressively increase, but growth rates in groups treated with Lv-shCUL4B-transduced cells were significantly slower than in controls (Lv-shCon, Figure 7A and B). Representative images of solid tumors are shown in Figure 7C. Compared to controls, tumor weights in groups treated with Lv-shCUL4B-transduced cells were reduced by 57.7% in U87 cell-implanted mice and 75.4% in U251 cell-implanted mice ($p < 0.01$, Figure 7D). These results further confirmed that knockdown of CUL4B could potently suppress glioma growth *in vitro* and *in vivo*.

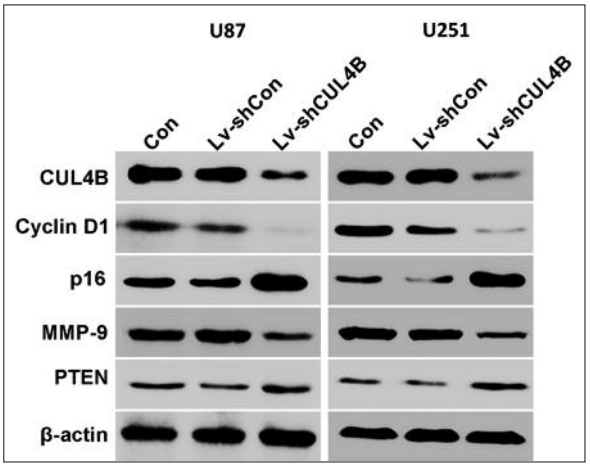

Figure 6. Cell cycle and migration regulatory proteins affected by depletion of CUL4B. Representative western blot showing expression alterations of cyclin D1, p16INK4a, MMP-9, and PTEN in uninfected and lentivirus-infected U87 and U251 cell lines. GAPDH protein was used as an internal control.

Discussion

Previous studies had shown that CUL4B is overexpressed in many types of solid tumors and contributes to epigenetic silencing of tumor suppressors. Knockdown of CUL4B reduced proliferation, colony formation, and invasiveness of hepatocellular carcinoma cells *in vitro* and inhibited tumor growth *in vivo*, effects that were attenuated by introduction of exogenous β-catenin[20]. Here, lentivirus-delivered shRNA targeting CUL4B was used to stably down-regulate its endogenous expression in glioblastoma cell lines U87 and U251 to ascertain the role of CUL4B in human glioma. Knockdown of CUL4B significantly inhibited proliferation and colony formation of both cell lines *in vitro*.

It had been shown that CUL4B is required to maintain cell cycle progression and that its targets include cell cycle-regulated proteins and DNA replication-related molecules[21,22]. Therefore, flow cytometry was used to analyze the effects of CUL4B knockdown on cell cycle control. The cell cycle was arrested at the G1 phase in U87 and U251 cells after CUL4B knockdown, which could contribute to the inhibition of cell proliferation. Our results are consistent with data of a previous study showing that the loss of CUL4B resulted in a significant reduction of cell proliferation and caused G1 cell cycle arrest, accompanied by upregulation of the cyclin-dependent kinase (CDK) inhibitors (CKIs) p21 and p57[23]. Here, knockdown of CUL4B decreased the expression of cyclin D1, a key regulator required for the G1-S transition, while increasing the level of p16INK4a that can directly inhibit the activity of cyclin D, thereby inhibiting S phase entry[24,25]. In addition, knockdown of CUL4B led to an increase in PTEN expression, which is known as a tumor suppressor implicated in a wide variety of human cancers[26]. While this implies an oncogenic role of CUL4B in glioma, its involvement in proteolysis of such tumor suppressors in glioblastoma cells needs to be confirmed by further investigation.

Moreover, it is noteworthy that CUL4B knockdown by shRNA markedly inhibited the growth of xenografts in nude mice, indicating that it

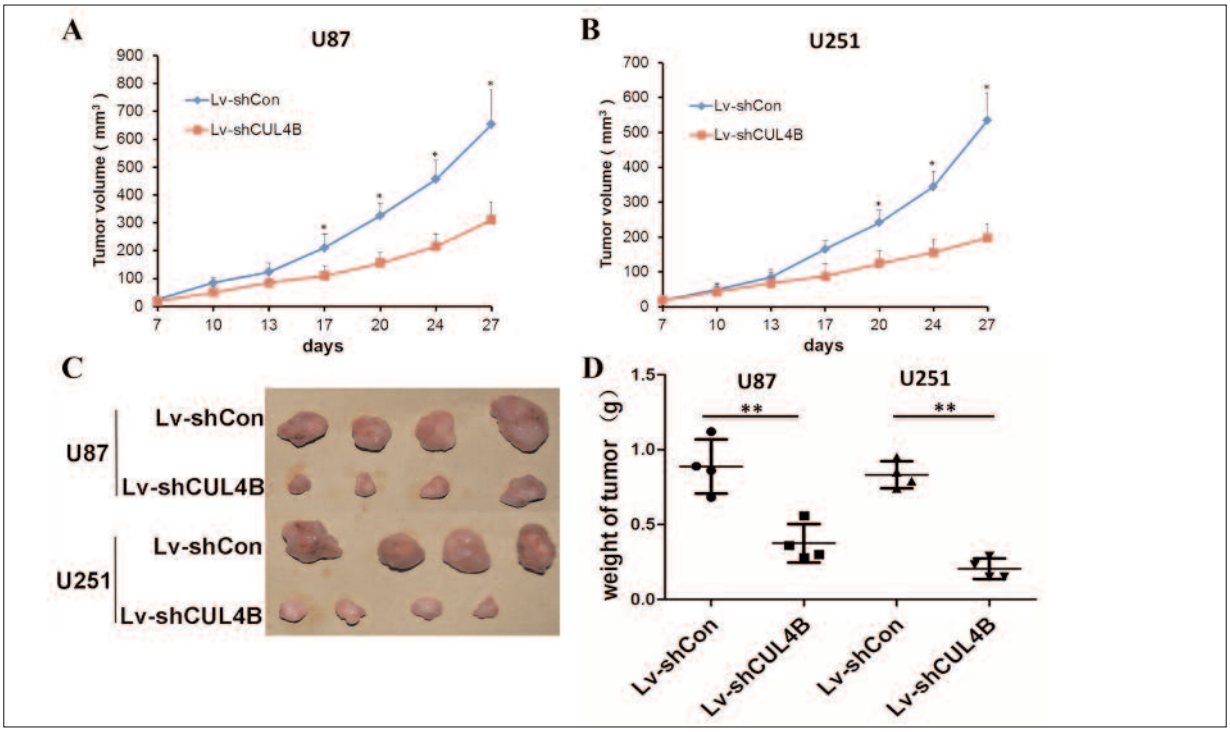

Figure 7. Tumor growth in glioma xenograft nude mice inhibited by depletion of CUL4B. ***A,*** and ***B,*** Growth curves of xenograft tumors in nude mice treated with lentivirus-infected U87 or U251 cells. (C) Representative light microscopy images of tumor sizes in nude mice. (D) Statistical analysis of xenograft tumor weights in nude mice treated with lentivirus-infected U87 or U251 cells. Data are mean ± SD. (n = 3; t-test). ** $p < 0.01$.

could alleviate glioma tumorigenesis *in vivo*. Additionally, knockdown of CUL4B impeded cell migration of U87 and U251 cells via suppression of MMP-9 that contributes to cell motility and invasiveness[27].

Conclusions

We have provided new evidence that CUL4B participates in malignant glioma proliferation *in vitro* and *in vivo*. Therefore, knockdown of CUL4B is likely to provide a novel alternative for targeted therapy of glioma and deserves further investigation.

Acknowledgements

This study was supported by National Natural Science Foundation of China (81172404, 81372720), Shandong Provincial Outstanding Medical Academic Professional Program and Special foundation for Taishan Scholars (No.ts20110814).

Conflict of Interest

The Authors declare that there are no conflicts of interest.

References

1) Zhu GY, Shi BZ, Li Y. FoxM1 regulates Sirt1 expression in glioma cells. Eur Rev Med Pharmacol Sci 2014; 18: 205-211.
2) Huse JT, Holland EC. Targeting brain cancer: advances in the molecular pathology of malignant glioma and medulloblastoma. Nat Rev Cancer 2010; 10: 319-231.
3) Chen SD, Hou PF, Lou L, Jin X, Wang TH, Xu JL. The correlation between MR diffusion-weighted imaging and pathological grades on glioma. Eur Rev Med Pharmacol Sci 2014; 18: 1904-1909.
4) Stupp R, Hegi ME, Mason WP, van den Bent MJ, Taphoorn MJ, Janzer RC, Ludwin SK, Allgeier A, Fisher B, Belanger K, Hau P, Brandes AA, Gijtenbeek J, Marosi C, Vecht CJ, Mokhtari K, Wesseling P, Villa S, Eisenhauer E, Gorlia T, Weller M, Lacombe D, Cairncross JG, Mirimanoff RO. Effects of radiotherapy with concomitant and adjuvant temozolomide versus radiotherapy alone on survival in glioblastoma in a randomised phase III study: 5-year analysis of the EORTC-NCIC trial. Lancet Oncol 2009; 10: 459-466.
5) Mirimanoff RO. High-grade gliomas: reality and hopes. Chin J Cancer 2014; 33: 1-3.
6) Qiu ZK, Shen D, Chen YS, Yang QY, Guo CC, Feng BH, Chen ZP. Enhanced MGMT expression

contributes to temozolomide resistance in glioma stem-like cells. Chin J Cancer 2014; 33: 115-122.

7) Lan L, Nakajima S, Kapetanaki MG, Hsieh CL, Fagerburg M, Thickman K, Rodriguez-Collazo P, Leuba SH, Levine AS, Rapic-Otrin V. Monoubiquitinated histone H2A destabilizes photolesion-containing nucleosomes with concomitant release of UV-damaged DNA-binding protein E3 ligase. J Biol Chem 2012; 287: 12036-12049.
8) Guerrero-Santoro J, Kapetanaki MG, Hsieh CL, Gorbachinsky I, Levine AS, Rapic-Otrin V. The cullin 4B-based UV-damaged DNA-binding protein ligase binds to UV-damaged chromatin and ubiquitinates histone H2A. Cancer Res 2008; 68: 5014-5022.
9) Ghosh P, Wu M, Zhang H, Sun H. mTORC1 signaling requires proteasomal function and the involvement of CUL4-DDB1 ubiquitin E3 ligase. Cell Cycle 2008; 7: 373-381.
10) Hu H, Yang Y, Ji Q, Zhao W, Jiang B, Liu R, Yuan J, Liu Q, Li X, Zou Y, Shao C, Shang Y, Wang Y, Gong Y. CRL4B catalyzes H2AK119 monoubiquitination and coordinates with PRC2 to promote tumorigenesis. Cancer Cell 2012; 22: 781-795.
11) Jiang T, Tang HM, Wu ZH, Chen J, Lu S, Zhou CZ, Yan DW, Peng ZH. Cullin 4B is a novel prognostic marker that correlates with colon cancer progression and pathogenesis. Med Oncol 2013; 30: 534.
12) Chen Z, Shen BL, Fu QG, Wang F, Tang YX, Hou CL, Chen L. CUL4B promotes proliferation and inhibits apoptosis of human osteosarcoma cells. Oncol Rep 2014; 32: 2047-2053.
13) Tarpey PS, Raymond FL, O'Meara S, Edkins S, Teague J, Butler A, Dicks E, Stevens C, Tofts C, Avis T, Barthorpe S, Buck G, Cole J, Gray K, Halliday K, Harrison R, Hills K, Jenkinson A, Jones D, Menzies A, Mironenko T, Perry J, Raine K, Richardson D, Shepherd R, Small A, Varian J, West S, Widaa S, Mallya U, Moon J, Luo Y, Holder S, Smithson SF, Hurst JA, Clayton-Smith J, Kerr B, Boyle J, Shaw M, Vandeleur L, Rodriguez J, Slaugh R, Easton DF, Wooster R, Bobrow M, Srivastava AK, Stevenson RE, Schwartz CE, Turner G, Gecz J, Futreal PA, Stratton MR, Partington M. Mutations in CUL4B, which encodes a ubiquitin E3 ligase subunit, cause an X-linked mental retardation syndrome associated with aggressive outbursts, seizures, relative macrocephaly, central obesity, hypogonadism, pes cavus, and tremor. Am J Hum Genet 2007; 80: 345-352.
14) Kerzendorfer C, Whibley A, Carpenter G, Outwin E, Chiang SC, Turner G, Schwartz C, El-Khamisy S, Raymond FL, O'Driscoll M. Mutations in Cullin 4B result in a human syndrome associated with increased camptothecin-induced topoisomerase I-dependent DNA breaks. Hum Mol Genet 2010; 19: 1324-1234.
15) Kerzendorfer C, Hart L, Colnaghi R, Carpenter G, Alcantara D, Outwin E, Carr AM, O'Driscoll M. CUL4B-deficiency in humans: understanding the clinical consequences of impaired Cullin 4-RING E3 ubiquitin ligase function. Mech Ageing Dev 2011; 132: 366-373.
16) Zhao Y, Sun Y. CUL4B ubiquitin ligase in mouse development: a model for human X-linked mental retardation syndrome? Cell Res 2012; 22: 1224-1226.
17) Lee J, Zhou P. Pathogenic Role of the CRL4 Ubiquitin Ligase in Human Disease. Front Oncol 2012; 2: 21.
18) Li X, Lu D, He F, Zhou H, Liu Q, Wang Y, Shao C, Gong Y. Cullin 4B protein ubiquitin ligase targets peroxiredoxin III for degradation. J Biol Chem 2011; 286: 32344-32354.
19) Vulto-van SA, Nakagawa T, Bahi-Buisson N, Haas SA, Hu H, Bienek M, Vissers LE, Gilissen C, Tzschach A, Busche A, Musebeck J, Rump P, Mathijssen IB, Avela K, Somer M, Doagu F, Philips AK, Rauch A, Baumer A, Voesenek K, Poirier K, Vigneron J, Amram D, Odent S, Nawara M, Obersztyn E, Lenart J, Charzewska A, Lebrun N, Fischer U, Nillesen WM, Yntema HG, Jarvela I, Ropers HH, de Vries BB, Brunner HG, van Bokhoven H, Raymond FL, Willemsen MA, Chelly J, Xiong Y, Barkovich AJ, Kalscheuer VM, Kleefstra T, de Brouwer AP. Variants in CUL4B are Associated with Cerebral Malformations. Hum Mutat 2014; 36: 106-117.
20) Yuan J, Han B, Hu H, Qian Y, Liu Z, Wei Z, Liang X, Jiang B, Shao C, Gong Y. CUL4B activates Wnt/beta-catenin signaling in hepatocellular carcinoma by repressing Wnt antagonists. J Pathol 2014; DIO: 10.1002/path.4492.
21) Miranda-Carboni GA, Krum SA, Yee K, Nava M, Deng QE, Pervin S, Collado-Hidalgo A, Galic Z, Zack JA, Nakayama K, Nakayama KI, Lane TF. A functional link between Wnt signaling and SKP2-independent p27 turnover in mammary tumors. Genes Dev 2008; 22: 3121-3134.
22) Hung MH, Jian YR, Tsao CC, Lin SW, Chuang YH. Enhanced LPS-induced peritonitis in mice deficiency of cullin 4B in macrophages. Genes Immun 2014; 15: 404-412.
23) Ji Q, Hu H, Yang F, Yuan J, Yang Y, Jiang L, Qian Y, Jiang B, Zou Y, Wang Y, Shao C, Gong Y. CRL4B interacts with and coordinates the SIN3A-HDAC complex to repress CDKN1A and drive cell cycle progression. J Cell Sci 2014; 127: 4679-4691.
24) Sherr CJ. The INK4a/ARF network in tumour suppression. Nat Rev Mol Cell Biol 2001; 2: 731-737.
25) Lowe SW, Sherr CJ. Tumor suppression by Ink4a-Arf: progress and puzzles. Curr Opin Genet Dev 2003; 13: 77-83.
26) Wan X, Helman LJ. Levels of PTEN protein modulate Akt phosphorylation on serine 473, but not on threonine 308, in IGF-II-overexpressing rhabdomyosarcomas cells. Oncogene 2003; 22: 8205-8211.
27) Aalinkeel R, Nair BB, Reynolds JL, Sykes DE, Mahajan SD, Chadha KC, Schwartz SA. Overexpression of MMP-9 contributes to invasiveness of prostate cancer cell line LNCaP. Immunol Invest 2011; 40: 447-464.